

A BAFFLE DESIGN FOR AN AIRGLOW PHOTOMETER ON BOARD THE KOREA SOUNDING ROCKET-III

YOUNG SUN LEE,¹ YONG HA KIM,¹ YU YI,¹ AND JHOON KIM²

¹Department of Astronomy and Space Science, Chungnam National University, Daejeon 305-764, Korea

²Korea Aerospace Research Institute, Daejeon 305-333, Korea

¹E-mail: leeyoungsun@hotmail.com, yhkim@cnu.ac.kr and euyiyu@cnu.ac.kr

(Received Dec. 5, 2000; Accepted Dec. 12, 2000)

ABSTRACT

A baffle system for an airglow photometer, which will be on board the Korea Sounding Rocket-III(KSR-III), has been designed to suppress strong solar scattered lights from the atmosphere below the earth limb. Basic principles for designing a baffle system, such as determination of baffle dimensions, arrangement of vanes inside a baffle tube, and coating of surfaces, have been reviewed from the literature. By considering the constraints of the payload size of the KSR-III and the incident angle of solar light scattered from the earth limb, we first determined dimensions of a two-stage baffle tube for the airglow photometer. We then calculated positions and heights of vanes to prohibit diffusely reflected lights inside the baffle tube from entering into the photometer. In order to evaluate performance of the designed baffle system, we have developed a ray tracing program using a Monte Carlo method. The program computed attenuation factors of the baffle system on the order of 10^{-6} for angles larger than 10° , which satisfies the requirements of the KSR-III airglow experiment. We have also measured the attenuation factors for an engineering model of the baffle system with a simple collimating beam apparatus, and confirmed the attenuation factors up to about 10^{-4} . Limitation of the apparatus does not allow to make more accurate measurements of the attenuation factors.

Key words : baffle, photometer, optical design, airglow

I. INTRODUCTION

A baffle system is to shield an optics from disturbing lights outside the field of view (FOV). The disturbing lights can be blocked and attenuated by wall reflection, by diffraction, by reflection at knife edge, or by combination of these attenuating means. Compared with the radiation from the sun, airglow, which arises mainly from discrete atomic and molecular transitions, is so weak that it is generally difficult to detect the airglow under the bright background radiation in the daytime. Since the Korea Sounding Rocket-III (KSR-III) will be launched in the daytime, a large amount of solar light scattered from the atmosphere below the earth limb could enter the photometer objective lens when the photometer aims at just above the limb. Thus, in order to obtain the required signal to noise ratio (S/N) under the circumstance that has bright unwanted lights in the vicinity, the control and suppression of stray lights are essential for the observation. A baffle system that can block the light outside the FOV is thus needed in front of the photometer objective lens. In this paper, we first reviewed principles and methods for designing several baffle systems from various literatures. By applying the appropriate designing method we designed a baffle sys-

tem for the KSR-III airglow photometer, and constructed an engineering model. We then described results of a Monte Carlo ray tracing simulation which we developed to evaluate performance of the designed baffle system. Finally we presented laboratory measurements of attenuation factors for the engineering model of the baffle system.

II. METHODS FOR DESIGNING A BAFFLE SYSTEM

Heinisch & Jolliffe (1971) have presented some basic principles of ray transfer processes which are crucial to designing a baffle system. First no optical components are permitted to view any sunlit wall or vane edge directly, that is, at least two reflections from darkened surfaces of the baffle tube or vanes are required between the stray light sources and the optical elements. Second, light from within the baffles is required to experience a maximum number of surface reflections from blackened surfaces before going into the objective lens. Third, a minimum number of vane edges should be directly exposed to the bright stray light. Finally, surfaces that are seen directly from the objective lens are to be finished with a black material. By applying these princi-

ples, we studied three kinds of baffle systems: a baffle tube with no vanes, baffles with vanes for diffuse reflection and for specular reflection.

(a) A Baffle Tube with No Vanes

As a starting design, we consider a baffle tube without vanes. We compute the amount of the irradiance arriving on a lens after being scattered on the wall of a baffle tube as a function of the incident angles with respect to the optical axis of a lens. Provided that the inner wall of the tube forms a diffusely reflecting cylinder, it is possible to derive an equation describing the diffusely reflected stray light reaching the lens when parallel beams of the solar light illuminate the tube with an angle (Wetherell, 1971). The geometry used for the calculation is illustrated in Fig. 1. Under these conditions the stray light irradiance on the lens, E_c , is given by

$$E_c = \frac{\rho E_i \sin \theta}{\pi} \int_0^{s_m} \frac{(L-s)(4s^2 - s^2 \tan^2 \theta)}{((L-s)^2 + a^2)^2} ds \quad (1)$$

where E_i is the solar irradiance normal to the line of sight, θ is the angle of the sun with respect to the optical axis, s is the distance from the front end of the tube, ρ is a diffuse reflectivity of the tube wall, L is the tube length, and a is the radius of the tube. For sunlight, $E_i=0.14 \text{ W/cm}^2$. Ratios of collected irradiance to incident irradiance (E_c/E_i) were computed and plotted as a function of the tube length to aperture diameter ratios in

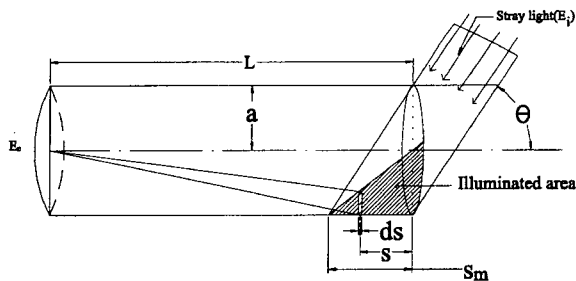


Fig. 1. Coordinates for equation (1).

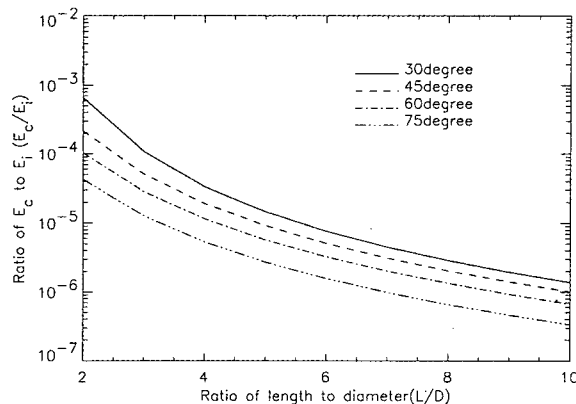


Fig. 2. Ratios of collected irradiance to incident irradiance as a function of length to diameter ratios for a baffle tube.

Fig. 2. In the cases examined, $\theta=30^\circ, 45^\circ, 75^\circ$ and $\rho=0.01$ are used. Fig. 2 demonstrates strong dependence of the collected irradiance on the length to diameter ratio as well as the incident angle. Doubling the ratio reduces the collected irradiance by more than an order of magnitude, confirming the conventional wisdom that a long baffle tube is desirable if possible.

(b) A Method for Erecting Vanes for Diffuse Reflection

Vanes are often used to reduce the amount of radiation that is reflected from walls in a baffle system. Although radiation reaching the lens can be attenuated by the wall of a baffle tube without vanes on it as much as an order of magnitude, as shown in Fig. 2, it is not sufficient to have such a baffle in front of the airglow photometer in which the baffle tube will be exposed to strong solar lights scattered from below the earth limb. Under this condition the internal walls of the tube must have vanes as shown in Fig. 3. The key to the efficient use of vanes is to arrange them such a way that no part of the lens can see a directly illuminated surface. The method of laying out a set of vanes has been illustrated, as in Fig. 3, by Smith (1990). The long dash-dotted line from the edge of the first vane to the rim of the lens indicates the necessary clearance space, into which the vanes cannot intrude without obstructing part of the radiation from the desired FOV. The height of the first vane is determined by the length and diameter of the tube and the FOV of the instrument. The second vane, the vane #2, is erected to the intersection of AB with the long dash-dotted FOV line. Solid line DC indicates the path of stray light from the opening of the first vane to the wall. The area from vane #2 to C is thus shadowed and safe for the lens to see. The vane #3 at the intersection of AC and the FOV line will prevent the lens from seeing the illuminated wall between the point C and the vane #3. This procedure is repeated until the entire side wall is protected. Note that the inside edges of the vanes should be sharpened and their surfaces should be roughened and blackened. Sandblasting to roughen the surface and blackening is usually a simple and effective treatment. For aluminum, black anodizing works well.

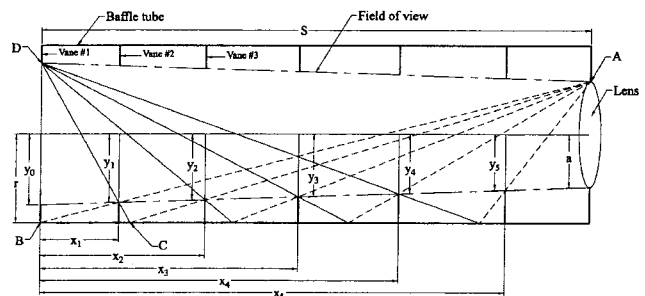


Fig. 3. A systematic layout for constructing vanes.

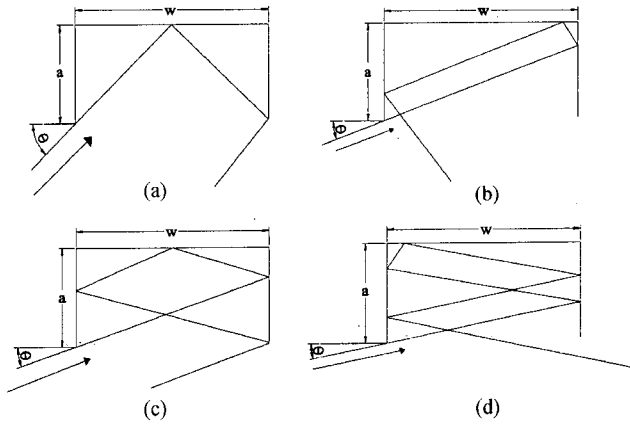


Fig. 4. Vane spacing for minimum number of specular reflections: (a) $2a/w > \tan\theta$ for two bounces, (b) $a/w > \tan\theta$ for three bounces, (c) $2a/3w > \tan\theta$ for four bounces, (d) $a/2w > \tan\theta$ for five bounces.

Positions and heights of the remaining vanes in the baffle tube are determined according to the geometry of the system. Using the geometry mentioned in the previous paragraph, the desired spacing between vanes and their heights can be calculated as follows (Bucsel, 1994). In Fig. 3, if the distance of vane #*n* from the outer end of the baffle tube is *x_n*, and the half-width of the entrance in vane #*n* is *y_n*, with *x₀*=0 and *y₀* denoting the values for the outermost vane, then equation

$$x_{n+1} = (y_0 - y_{n+1}) \frac{s}{y_0 - a} \tag{2}$$

$$y_{n+1} = r - \frac{r + a}{1 + z_n} \tag{3}$$

where,

$$z_n = 2a \left[r - r_0 + x_n \frac{y_0 - a}{s} \frac{y_0 + r}{y_0 + y_n} \right]^{-1} \tag{4}$$

The radius of the lens is *a* and the radius of the baffle tube is *r*. The objective lens is located at a distance, *s*, from the outermost vane. Beginning from the outermost vane, subsequent vane positions and heights are determined until *x_n* becomes greater than *s*. Under this kind of arrangement, stray light is forced to be reflected at least twice within the baffle tube.

(c) A Method for Erecting Vanes for Specular Reflection

In order to reduce stray light in an optical system, one of the designer’s goals is to force the light to make a maximum number of reflections or scatterings off from absorbing surfaces before reaching the lens. Using this concept, arrangements of vanes for controlling specular reflections will be discussed in this section. For instance, with reflectivity $\rho=0.1$, we have attenuation $a=(0.1)^n$ after *n* bounces, and *n* can be made almost as large as we would like to by a proper design of the baffle sys-

tem. In Fig. 4, criteria, adopted from Freniere (1980), are shown for determining vane spacing when we wish a ray at an input angle θ to undergo a given number of specular reflections before leaving the wall. The criteria are useful only if both vanes and baffle tube walls are highly specularly reflecting. Indeed, the number of specular reflections can be made arbitrarily large; one way that this can be done is by increasing the ratio of *a* to *w* shown in Fig. 4. This approach neglects scattering from vane edges. The configuration in Fig. 4 is derived from the requirement that no first specular reflections from the baffle reach the objective lens. This arrangement is a vast improvement over a plain tube, and if specularly reflecting finish is applied to that baffle system, it may be all that is needed. In Fig. 3, the vanes are spaced so that no first diffuse reflections from the baffle reach the objective lens; an alternate way of stating this requirement is that the objective lens can only see portions of the baffle that are not directly illuminated, except for vane edges. When the baffle system has a diffusely reflecting surface, an optimum vane placement is more difficult to determine than when the finish is specularly reflecting. One cannot guarantee more than two bounces from a diffusely reflecting baffle before striking the objective lens.

(d) Scattering from Vane Edges

The designer must consider the scattering of light from the edges of vanes in designing a baffle system. Since the main sources of stray light in the baffle tube can be the knife edges of vanes that almost touch the FOV line, the safety margin between the acceptance cone of the FOV and the edges of vanes should be assigned. A typical value for the scattering coefficient of a sharp black edge is $S=1.5 \times 10^{-4} \text{ cm sr}^{-1}$, which corresponds to diffuse scattering from a strip with a thickness of 0.1 mm and a reflectivity of 0.05 (Leinert & Klupperlberg, 1974). It is noted that the positioning of the bevel on the vane edges varies with the location of the vanes in the system (Breault, 1977). That is, in the front section of a baffle system the bevel should be on the object side of the vanes as described in the Fig. 5(a); the side that will receive direct radiation from the off-axis source. The bevel should be on the opposite

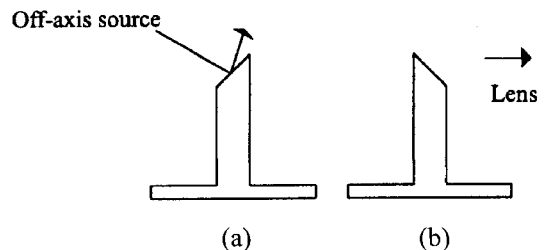


Fig. 5. Directions of vane edge(bevel).

side at locations deeper into the system where direct radiation from the unwanted source can be prevented from reaching the beveled edge as in the Fig. 5(b). For the systems where the edge scatter is significant, its effect can be minimized in the manners such as removing the vane edges from the FOV of the objective lens, reducing the edge radius and changing the coating, etc..

III. DESIGN OF A BAFFLE SYSTEM

We have designed a baffle system that can be best performed for the airglow photometer by adopting merits in design techniques described in the previous section.

(a) Description of a Baffle System

Although the longer length of the baffle tube will guarantee the higher attenuation of stray light, the total length of the baffle tube and the photometer is limited by the inner diameter 76 cm of the KSR-III payload section. And yet it is required that any part of the objective lens must not see directly the earth limb that is 10.1° below the horizontal direction at an altitude of 100 km. The baffle tube length, L , is approximately estimated by

$$L > \frac{D}{\theta} \quad (5)$$

where D is the lens diameter, and θ is the angle between the limb and the optical axis (Bucsele, 1994). For our airglow measurements during the daytime, the solar light scattered from the atmosphere below the limb is extremely bright in comparison with the airglow emission that we want to measure. It is thus required to remove the bright stray light from the lower atmosphere outside the FOV to a high degree before entering the photometer objective lens. We adopt a two stage baffle system that can reject such bright stray lights with two successive baffles. The front baffle plays a role of blocking direct light from below the limb and the rear baffle then rejects or attenuates the remaining stray light that is being reflected from the walls of the front baffle. The stray light outside the FOV is more serious in the vertical direction than the horizontal direction as our photometer looks horizontally during the vertical flight of the KSR-III. Thus, we adopt a rectangular FOV with 1° in vertical by 4° in horizontal direction. The airglow photometer has a quartz plano-convex objective lens with an effective aperture of 15 mm and a back focal length of 46 mm. A slit of 0.8×3.2 mm on the focal plane of the objective lens defines the FOV of $1^\circ \times 4^\circ$. For the baffle design, safety margins of 1.5° for vanes and 0.25° for the outermost vanes of the rear baffle are added to the photometer's FOV to reduce the edge scattering.

(b) Determining Dimensions of the Baffle Tube

Given the diameter of the KSR-III, the angle of the earth limb, and the FOV of the instrument, the dimensions of the two-stage baffle tube are determined as follows. In Fig. 6, α is the half of the FOV, α is the maximum allowed angle from the optical axis. The maximum allowed angle should point above the earth limb to prohibit the bright scattered light from entering into the second stage baffle. D_1 is the effective diameter of the lens, D_2 is the diameter of the first vane in the second stage baffle tube, and D_3 is the diameter of the first vane in the first stage baffle tube, x_1 and x_2 are the length of the second and first stage baffle tube, respectively. Among these parameters, the following relationships can be derived from the geometry of Fig. 6.

$$x_1 = \frac{D_1}{\tan \beta - \tan \alpha}, \quad D_2 = \frac{\tan \beta + \tan \alpha}{\tan \beta - \tan \alpha} D_1 \quad (6)$$

$$x_2 = \frac{\tan \beta + \tan \alpha}{(\tan \beta - \tan \alpha)^2} D_1, \quad D_3 = \frac{(\tan \beta + \tan \alpha)^2}{(\tan \beta - \tan \alpha)^2} D_1 \quad (7)$$

$$L = x_1 + x_2 = \frac{2D_1 \tan \beta}{(\tan \beta - \tan \alpha)^2} \quad (8)$$

Dimensions of the baffle tubes as listed in Table 1 are determined from these relations with $D_1=15$ mm, $\alpha_v=2^\circ$ for the vertical direction, $\alpha_h=3.5^\circ$ for the horizontal direction and the limb angle $\beta=7.3^\circ$. For both vertical and horizontal directions, a safety margin of 1.5° was added to the half angles of the intended FOV to prohibit light scattered from the edges of vanes from entering into the photometer's FOV. Since the whole length of the baffle tube can not be longer than 445 mm, the maximum allowed angle of 7.3° was adopted from the geometry requirement. The vertical dimension of 150 mm for the space assigned to our instrument in the KSR-III provides a sufficient margin for the baffle tube diameter of 95 mm.

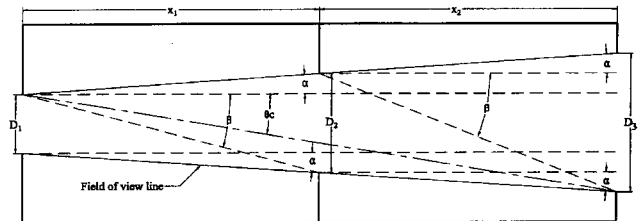


Fig. 6. Geometry for optimizing the baffle tube length.

Table 1. Optimized dimensions of the baffle tube

Semi-FOV	x_2	x_1	D_3	D_2
Vertical $\alpha_v=2^\circ$	281.6	161.0	46.0	26.0
Horizon $\alpha_h=3.5^\circ$	633.0	224.0	119.0	42.4

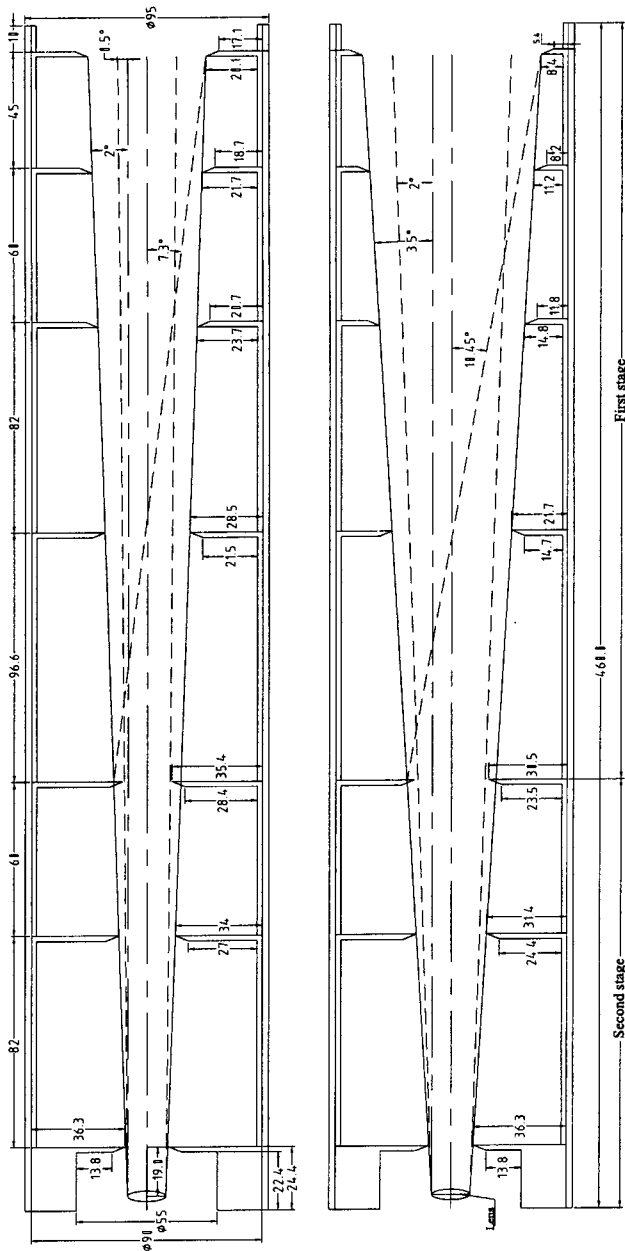


Fig. 7. Side view of the baffle system; the left and right ones are for the vertical and horizontal planes, respectively.

(c) Erecting Vanes

After adopting the dimensions of the first and second stage baffle tubes, the heights of the outermost vane are calculated with maximum allowed angles, β , of 7.3° and 10.5° for vertical and horizontal directions, respectively. The maximum allowed angle for the horizontal direction is not critically constrained because stray lights are distributed homogeneously along the azimuthal plane, while stray lights increase very abruptly with depression angles in the vertical direction. The positions of inner vanes are determined with the requirement of the case (b) in Fig. 4, which makes rays reflect more than three times between the subsequent vanes. Since the maxi-

imum allowed angle is larger for the horizontal direction than the vertical direction, the distance between vanes is required to be shorter for the horizontal plane than the vertical plane of the baffle tube. In order to make the vane structure as simple as possible, we adopt the shorter spacing between vanes with different heights for the two planes, which satisfies the requirement for both directions. The heights of vanes are constrained by limiting lines for the safety margin added FOV, as shown in Fig. 7. The height on the vertical plane is always taller than that on the horizontal plane for each vane, and thus the shape of clearance above each vane inside the circular baffle tube is elliptical when viewed from the front of the baffle. Note in Fig. 7 that the tip of the outermost vane in the second stage baffle is above the line that marks the safety margin added FOV, but little below the line that marks the instrument's FOV. This arrangement is to reduce residual stray light from the first to the second stage of the baffle system.

(d) Anodizing the Baffle System

Stray light reflected inside a baffle system is usually suppressed by black surfaces. The surface coating on the baffle system is thus a key factor contributing to performance. Unfortunately, the well known coating materials, such as 3M Black Velvet paint, Martin Black and Parsons Black with a low reflectivity (Joseph & David, 1993), are not available in Korea. Commonly available black anodizing treatment is thus applied to all the parts in our baffle system before being assembled. The reflectivity of a surface treated by black anodizing is not known in a standard way and is expected to vary with detail method of treatments. In our laboratory we estimated the reflectivity of a few percent for the anodized surface of our baffle system.

IV. PERFORMANCE EVALUATION OF THE BAFFLE SYSTEM

(a) Evaluation by a Ray Tracing Program

Performance of a baffle system can be evaluated by calculating attenuation factors as a function of incident angles for entering light with respect to the optical axis. We have developed a ray tracing program that utilizes the Monte Carlo method to simulate diffuse scattering from the surface of the baffle. The program traces a ray scattering multiple times from an entering point to an exiting point, with an assumption that the ray always stays in a vertical plane to the scattering surface. Every time a ray is scattered off the surface, a random number determines a scattering angle to redirect the ray. The program follows 20,000 entering rays with a given incident angle until each ray is scattered nine times or exits from the baffle system. Since clearance above the vanes

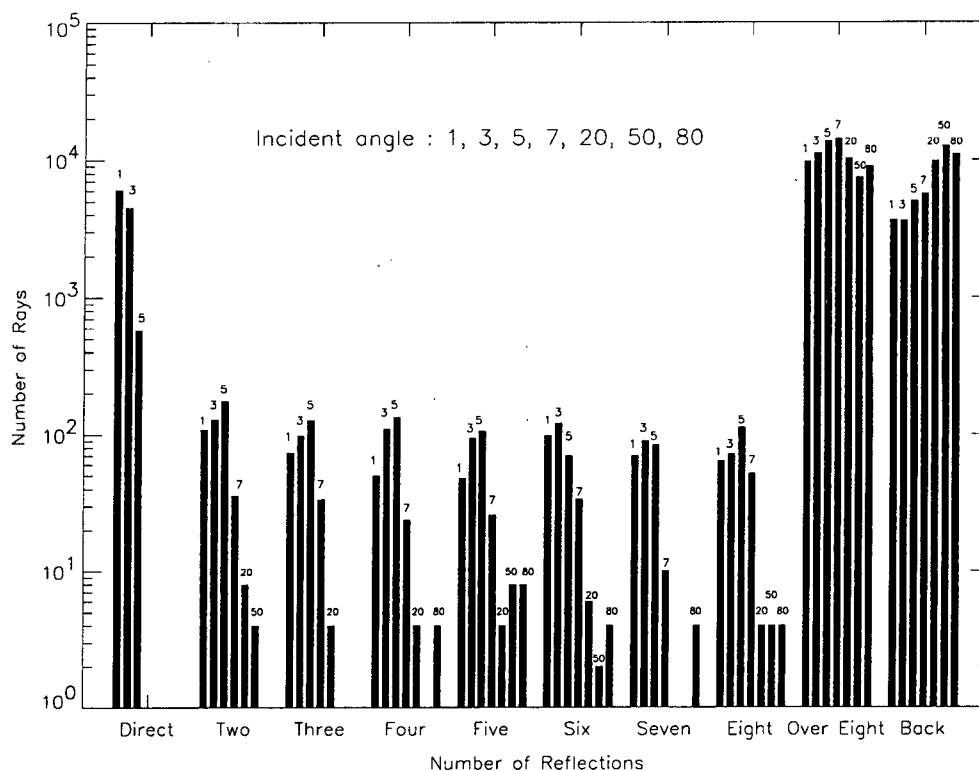


Fig. 8. The number of rays entering the lens after being reflected one, two, three, four, five, six, seven, eight, and more than nine times for various incident angles.

inside the baffle tube is elliptical, the program distributes the 20,000 entering rays over one quadrant of the elliptical clearance above the outermost vane. Fig. 8 shows the number of rays reaching the objective lens (the exit aperture of the baffle) after being scattered two, three, four, five, six, seven, and eight times. About half the rays do not reach the objective lens after more than eight times of scattering, and the considerable number of rays are back-scattered toward the entering clearance of the baffle. There is no ray outside the FOV that bounces one time to enter the objective lens, as the arrangement of vanes guarantees. Fig. 8 indicates that very small number of rays can intrude into the lens after bouncing two times for incident angles of more than 7° , although the arrangement of vanes is expected to make rays reflect more than two times, as shown in Fig. 4(b). This is because rays are reflected to random directions, rather than in specular direction, in the simulation.

Attenuation factors are computed by multiplying the reflectivity, ρ , of the surface everytime scattering occurs in the simulation. Fig. 9 shows attenuation factors as a function of the incident angles for assumed reflectivities of 0.03 and 0.05. For Fig. 9 it is assumed that all the rays scattering more than five times enter the lens after being attenuated by a factor of ρ^5 . Fig. 9 indicates that the attenuation factor decreases very abruptly near the critical angles θ_c (see Fig. 6), 4.3° and 5.9° for the vertical and horizontal directions, respectively. This is because

rays with incident angles greater than the critical angles can not reach directly the lens, as shown in Fig. 6. The attenuation factor outside the critical angles stays between 10^{-5} and 10^{-7} , with difference of a factor of about 10 for two assumed reflectivities. The simulation, therefore, indicates that our design goal for the baffle system with an attenuation factor less than 10^{-6} can be achieved if the surface reflectivity is 0.03 or less.

(b) Evaluation by Laboratory Measurements

Performance test of the baffle system has been carried out to estimate the attenuation factors as a function of incident angles. In order to measure the attenuation factors, the photometer with the baffle system is placed on a rotatable platform in front of a collimator. The collimator produces a collimated beam with a diameter of 150 mm from a six inch Zeiss refracting telescope that has a point light source installed on its focal point. The photometer's signals are recorded for angles from 0° to 10° with respect to the collimated beam. The attenuation factor for an incident angle is estimated by normalizing the measured value at the angle with the value measured at 0° . Since both the FOVs of the photometer's slit and the critical angles of the baffle system are different for vertical and horizontal directions, the measurements were carried out separately for each direction. Fig. 10 shows the measured attenuation factors up to 10° with asterisks and diamonds for the cases with and

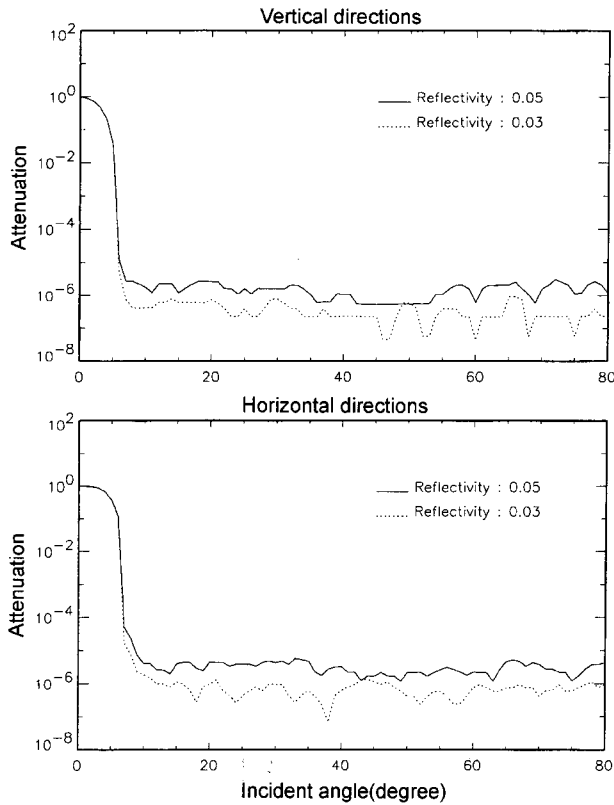


Fig. 9. Attenuation factors for vertical and horizontal directions with assumed reflectivities of 0.03 and 0.05.

without the baffle system in front of the photometer, respectively. The computed attenuation factors, also shown with solid lines, are larger than the measured ones up to 5° for the vertical direction and 6° for the horizontal direction since the computed values are for the baffle system only, not reduced by the photometer's field limiting slit. The baffle system appears to reduce the attenuation factors by a factor of about 100 just outside the FOV of the photometer.

However, the attenuation factors do not decrease at angles larger than 6° for the vertical direction and 7° for the horizontal direction to the level of the computed values. This is probably because the dynamic range of the measurements is not sufficiently wide to obtain meaningful results at the level of 10^{-5} . The dynamic range of the current measurement method depends on several factors, such as dark counts of the photometer, off-axis irradiance of the collimator, and others. Among these factors, the off-axis irradiance from the collimator in our measuring apparatus is particularly serious because we use a conventional telescope as a collimator. Bucsella (1994) carried out similar measurements down to the level of about 10^{-4} for the attenuation factor. In order to verify whether the baffle system achieves the attenuation factor of 10^{-6} , very sophisticated measuring apparatus or actual rocket flight experiment is needed.

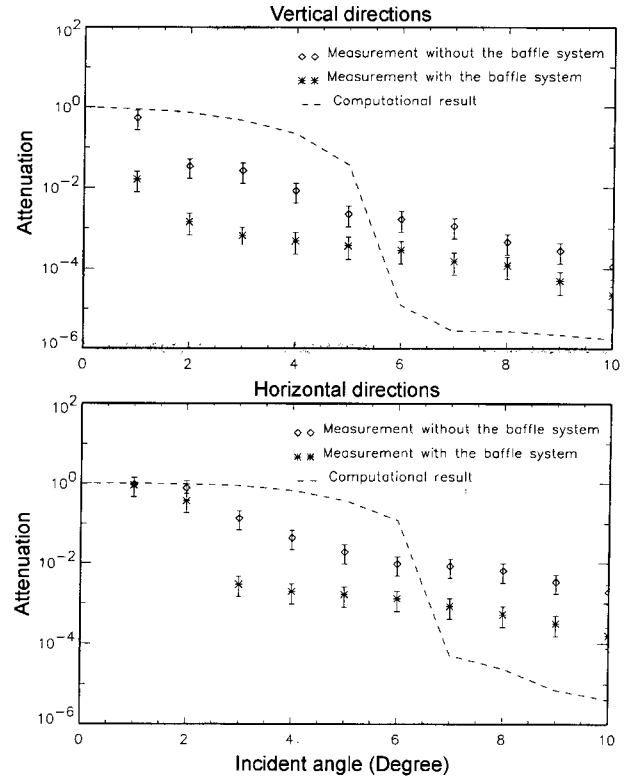


Fig. 10. Comparison of computed attenuation factors with measured ones. The asterisk and diamond signs with error bars indicate the measured attenuation factors.

V. CONCLUSIONS

A baffle system for the KSR-III rocket airglow photometer has been designed to suppress strong solar scattered lights from the atmosphere below the earth limb. Basic principles for designing a baffle system, such as determination of baffle dimensions, arrangement of vanes inside a baffle tube, and coating of surfaces, have been reviewed from the literature. By considering the constraints of the payload size of the KSR-III and the incident angle of solar light scattered from the earth limb, we determined dimensions of a two-stage baffle tube for the airglow photometer. We calculated positions and heights of vanes that block the diffusely reflected lights from the baffle tube surface. The performance of the designed baffle system was evaluated by a ray tracing program that we developed using a Monte Carlo method. The attenuation factors of the baffle system are computed to be on the order of 10^{-6} for angles larger than 10° , which satisfies the requirements of the KSR-III airglow experiment. We have also measured the attenuation factors for an engineering model of the baffle with a simple collimating beam apparatus, and confirmed the attenuation factors up to about 10^{-4} in the vertical direction. Limitation of the measuring apparatus prohibited more accurate measurements of the attenuation factors.

YHK was supported in part by KOSEF grant (1999-1-113-001-5). This work was supported by KARI(Korea Aerospace Research Institute) KSR-III project.

REFERENCES

- Breault, R. P. 1977, SPIE, 107, 3
Bucsele, E. J. 1994, Ph. D. Dissertation, The University of Michigan
Freniere, E. F. 1980, SPIE, 257, 19
Heinisch, R. P. and Jolliffe, C. J. 1971, Applied Optics, 10, 2016
Joseph S. A. and David L. S. 1993, The infrared and electro-optical systems handbook, c1993, SPIE Optical Engineering Press
Leinert, C. and Kluppelbery, D. 1974, Applied Optics, 13, 556
Smith, W. J. 1990, Modern Optical Engineering, McGraw-Hill, New York
Wetherell, W. B. 1971, Final report on NASw-2174, 60